

## Thesis Changes Log

**Name of Candidate:** Maksim Zakharkin

**PhD Program:** Materials Science and Engineering

**Title of Thesis:** NASICON-type  $\text{Na}_{3+x}\text{Mn}_x\text{V}_{2-x}(\text{PO}_4)_3$  cathode materials for sodium-ion batteries

**Supervisor:** Prof. Keith Stevenson

*The thesis document includes the following changes in answer to the external review process.*

The author would like to express his gratitude for the useful comments and questions from the reviewers.

## Prof. Stanislav Fedotov

Several comments appeared while carefully reading the thesis which should be addressed:

### Comment 1

In the literature overview the author primarily focuses on the structural aspects of  $\text{Na}_3\text{M}_2(\text{PO}_4)_3$  stoichiometry but it is highly recommended to provide a more generalized and detailed description of the NASICON structure and its peculiarities to guarantee further understanding of other stoichiometries with different sodium content which appear throughout the manuscript as well as for the better comprehension of the de/insertion mechanism studied by operando diffraction.

### Reply 1

- The author thanks the reviewer for constructive comment. A more generalized and detailed description of the NASICON structure was provided.

Chapter 2.3.2. was corrected as follows:

*$A_y\text{M}_2(\text{XO}_4)_3$  (A: generally an alkali metal, but also Mg, Zn, etc. and their combinations are known; M: either a single or a combination of transition metals or elements like Sn, Ge, Sc, Mg, etc.; X: mainly P, Si as well as W, Mo, S, As, etc.;  $0 \leq y \leq 5$ ) compounds are studied as prospective superionic conductors and electrode materials in metal-ion batteries. Compounds  $\text{Na}_y\text{M}_2(\text{PO}_4)_3$  were first reported in the 1880s, [ ] then again in the 1960s [ ] and a mineralogical example kosnarite was described in 1993 [ ].*

A comparison between NASICON and anti-NASICON phases was moved from the Chapter 2.3.3. to the Chapter 2.3.2.

Chapter 2.3.2. was expanded as follows:

*In the NASICON framework three independent sites can be occupied by alkali ions. The first one is an octahedral A1 position located between the lower and upper  $\text{MO}_6$  octahedra of neighboring "lantern"*

units, which form infinite columns of  $[O_3AlO_3MO_3AlO_3]$  along  $c$ -axis. These columns are connected by three  $XO_4$  tetrahedra in such a way that empty trigonal prisms are created in the center of the  $M_2(XO_4)_3$  "lantern" units. The second site is located in an eight-fold A2 position between these infinite columns. Together they form the 3D framework, which leads to the crystallographic formula  $(A1)(A2)_3M_2(XO_4)_3$  (Fig. 2. 1 left). The third site is an octahedral A3 position located between  $MO_6$  octahedra inside the  $M_2(XO_4)_3$  "lantern" unit resulting in  $(A1)(A2)_3(A3)M_2(XO_4)_3$  or  $A_5M_2(XO_4)_3$ . Its filling is energetically unfavorable due to the great Coulombic repulsion.

Therefore, the lattice may be described as composed of infinite  $[O_3AlO_3MO_3AlO_3]$  columns parallel to the  $c$ -axis linked by  $PO_4$  tetrahedra placed perpendicularly to the  $c$ -direction []. The A1 position is located within the columns. The A2 position is situated between the columns above the  $PO_4$  tetrahedra. Then, the  $a$ -parameter is directly related to the column diameter (i.e. a function of the  $M^{n+}$  radius) as well as to the inter-column distance (i.e. a function of the occupancy of the A2 positions). The  $c$ -parameter is influenced by the competition between several interactions summarized in Fig. 2. 1 right:

- the  $M^{n+}$  radius
- the  $M^{n+}-M^{n+}$  electrostatic repulsions
- the  $O^{2-}-O^{2-}$  repulsions occurring when the A1 position is empty
- the  $A^+(A1)-O^{2-}$  attractions
- the  $A^+(A1)-M^{n+}$  repulsions through the shared faces

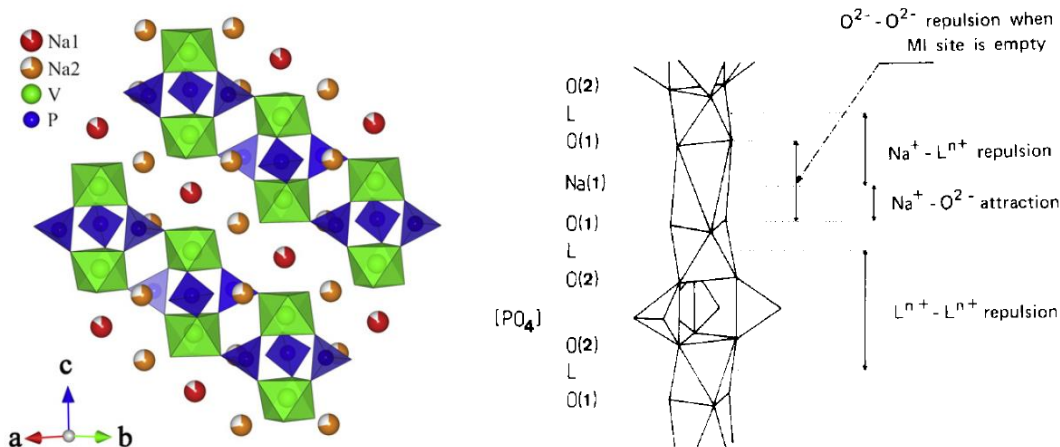


Fig. 2. 1 The NASICON framework of the  $Na_3V_2(PO_4)_3$  described as array of parallel columns linked by  $PO_4$  tetrahedra [] (left), Electrostatic interactions within a column of the NASICON-type  $Na_3L_2(PO_4)_3$  [] (right)

It should be noted that in the case of  $M^{3+}$  the obtained  $Na_yM_2(PO_4)_3$  compounds would have  $Na_3M_2(PO_4)_3$  composition. Partial substitution of  $M^{3+}$  by  $x$  moles of  $M^{2+}$  would require filling of A sites with sodium ions, therefore compositions of  $Na_{3+x}M'_xM_{2-x}(PO_4)_3$  will be reached. Similarly, deintercalation of  $x$  moles of sodium from  $Na_3M_2(PO_4)_3$  would induce  $M^{3+}$  to  $M^{3+x/2}$  redox transition and  $Na_{3-x}M_2(PO_4)_3$  will be obtained.

## Comment 2

There is some misattribution of the terms and names of minerals when the author describes the  $AMPO_4$  family of electrode materials. A correct classification of the olivine/triphylite/maricite-type structures and their features description should be made. I recommend to read and refer to the paper of M. Avdeev, Inorg. Chem., 2013 (10.1021/ic400870x).

## Reply 2

- The author agrees with the reviewer. The misattribution was corrected and the structural features were additionally highlighted.

### Comment 3

3. When dealing with particle sizes from SEM/TEM micrographs the histograms of particle size distribution should be made using graphical analyzing software, i.e. ImageJ. The average particle sizes is recommended to extract from such histograms but not visually (“by eye”).

### Reply 3

- the histogram of the particle size distribution was made using the ImageJ software. The observed mean particle size lies in the range of 350-480 nm. Therefore the value of the characteristic diffusion length for the diffusion coefficient calculations is close to the used 200 nm.

The data was added to the Appendix A

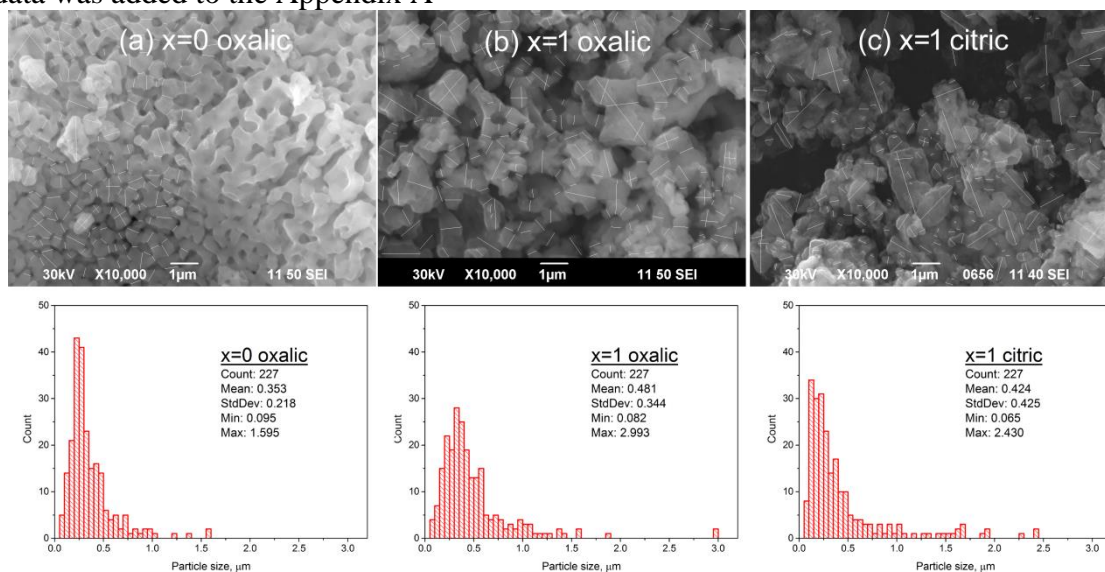


Fig. A 1 SEM images and the histograms of the  $Na_{3+x}Mn_xV_{2-x}(PO_4)_3$  particle size distributions derived with the ImageJ software [ ] (a)  $x=0$ , synthesized with oxalic acid, (b)  $x=1$ , synthesized with oxalic acid, (c)  $x=1$ , synthesized with citric acid.

### Comment 4.1

4. A more detailed explanation on why for the structural analysis the samples obtained by citric methods were used, but for electrokinetic parameters analysis the oxalic method was utilized for sample preparation.

### Reply 4.1

- The histogram of the particle size distribution for oxalic- and citric-based samples was made using the ImageJ software. As explained in the manuscript the citric-based samples show a higher tendency for the agglomeration of primary particles and considerably higher amount of large particles, which may be associated with a shoulder on the cathodic peak.

The data was added to the Appendix A and to the Chapter 4.

The samples made with citric acid as a reducing agent show higher amount of large particles (Fig. A 1 b and c), which may be associated with a shoulder on the cathodic peak (Fig. 4. 1 right).

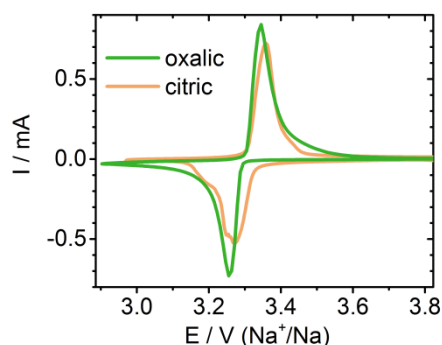


Fig. 4. 1 CVs of  $\text{Na}_3\text{V}_2(\text{PO}_4)_3$  electrodes: oxalic-based samples with glucose-derived coating and citric-based samples without additional carbon coating. Scan rate is  $0.2 \text{ mV s}^{-1}$ .

### Comment 4.2

Do the samples prepared using oxalic approach demonstrate the same structural behavior and de/intercalation mechanism in the operando experiments as citric ones?

### Reply 4.2

- The samples prepared with oxalic acid show very similar unit cell parameters. The electrochemical signatures such as the shape of galvanostatic curves also reproduce the ones by the citric-based samples.

One distinction can be noted, which was added to the Chapter 7.

*We note that although structural studies of citric-based samples ([1]) imply the formation of an intermediate  $\text{Na}_2\text{M}_2(\text{PO}_4)_3$  phase during charge and discharge and, correspondingly, two biphasic processes in the 2.5-3.8 V range, the operando X-ray diffraction, CV and chronoamperometry data obtained with oxalic-based samples do not allow to distinguish between these processes (Fig. 6. 1 right).*

- We performed operando XRD experiments with the oxalic-based  $\text{Na}_3\text{V}_2(\text{PO}_4)_3$  and updated the Fig. 6.3 with the new data.

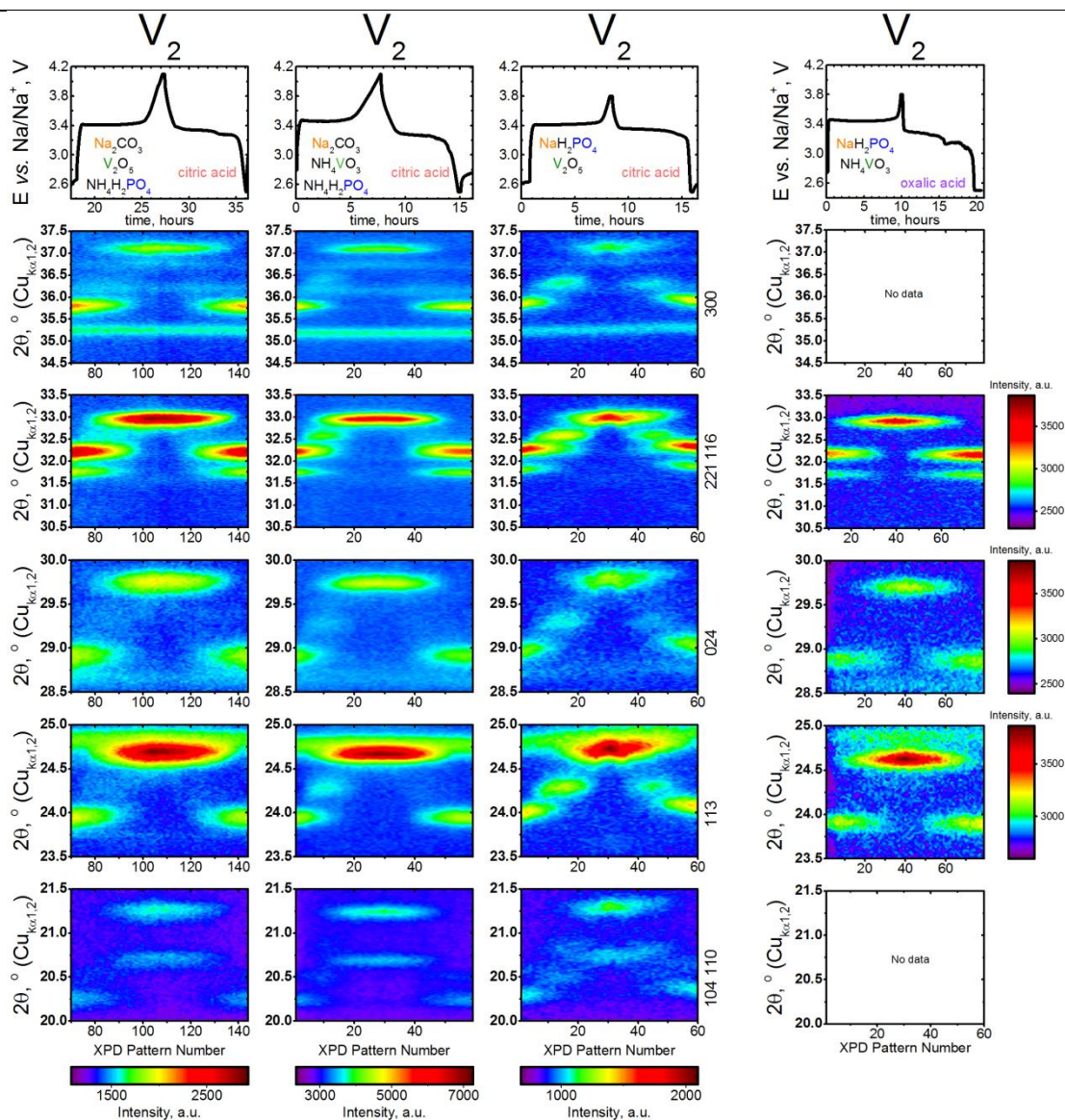


Fig. 6. 1 Transformations of the selected regions ( $20.0-21.5^\circ$ ,  $23.5-25.0^\circ$ ,  $28.5-30.0^\circ$ ,  $31.5-33.5^\circ$ ,  $34.5-37.5^\circ$ ,  $Cu_{K\alpha 1/K\alpha 2}$ ) of XRPD patterns during operando charge-discharge in the 2.5-3.8V and 2.5-4.1V voltage windows for  $Na_3V_2(PO_4)_3$ , synthesized by the same procedure, but using different precursors, which are specified on the top graphs.

- The observed differences may be related to faster kinetics for the oxalic-based materials or may be related to the different size of the coherently scattering regions of the “ $Na_2V_2(PO_4)_3$ ” nuclei.

### Comment 5

Why 0.5 M  $NaPF_6$  electrolyte was used for the study of the electrochemical properties in Na cells but not 1M?

### Reply 5

- The use of the 0.5 M  $NaPF_6$  electrolyte was caused by temporary constraints to completely dissolve 1 mole of  $NaPF_6$  in solvents without precipitation.

### **Comment 6**

Please do not use informal reduced forms of auxiliaries like “don’t” or “doesn’t” (pp. 28, 78, 86, 93).

### **Reply 6**

- The reduced forms of auxiliaries were corrected.

### **Comment 7**

The manuscript contains some technical misprints:

- a. perspective → prospective (adj., p. 29)
- b. *R-I* → *P-I* (p. 46)
- c. BC/AB/CA → AB/BC/CA (p. 26)
- d.  $dQ/dV$  →  $dQ/dE$  (p. 69 and after)

### **Reply 7**

- The misprints were corrected

## **Prof. Eugene Goodilin**

---

As a small set of questions to briefly discuss during the defense procedure, I would like to post the following:

### **Comment 8**

How trustable is the initial reagent weight compositions? Usually it is not safe to trust formulas of manufacturers and it is better to pre-analyze the precursors, probably it would reduce the deviations from the expected values in Fig.4.3 and improve the final phase assemblage.

### **Reply 8**

- The author thanks the reviewer for this comment. The initial reagents supplied by Sigma-Aldrich were used as-received taking the indicated compositions for granted. The deviations from the expected values in Fig. 4.3 indeed may be related to the differences between the real and anticipated compositions. The major deviations in composition are related to sodium content. As a sodium precursor  $\text{Na}_2\text{CO}_3$  was mainly used. This reagent may be hydrated and its pre-analysis by *e.g.* TGA may help timely take account of the possible deviations from the expected valued. However, our experimental results did not show the presence of impurities induced by insufficient sodium content. Also, while the EDX results underestimated Na content, the ICP results overestimated Na content. Na content can be underestimated by EDX due to partial absorption of Na X-rays by the sample. Overestimation by ICP is on the order of several percent. Our electrochemical data suggests that almost 2 sodium ions can be extracted from  $\text{Na}_3\text{V}_2(\text{PO}_4)_3$  and inserted back with high coulombic efficiency values approaching 100%. Based on the whole set of data we conclude that the real elemental composition in the obtained samples is very close to the anticipated values, though the author agrees that precursor pre-analysis is a useful habit.

### Comment 9

Precipitation methods usually guaranty no phase and compositional uniformity of muticomponent precursors (especially if they are performed dropwise) because sedimentation of each component would occur separately at its own critical concentration of salts (added ions). Could it have any influence on the final product uniformity? What could be used to improve the initial precursor uniformity?

### Reply 9

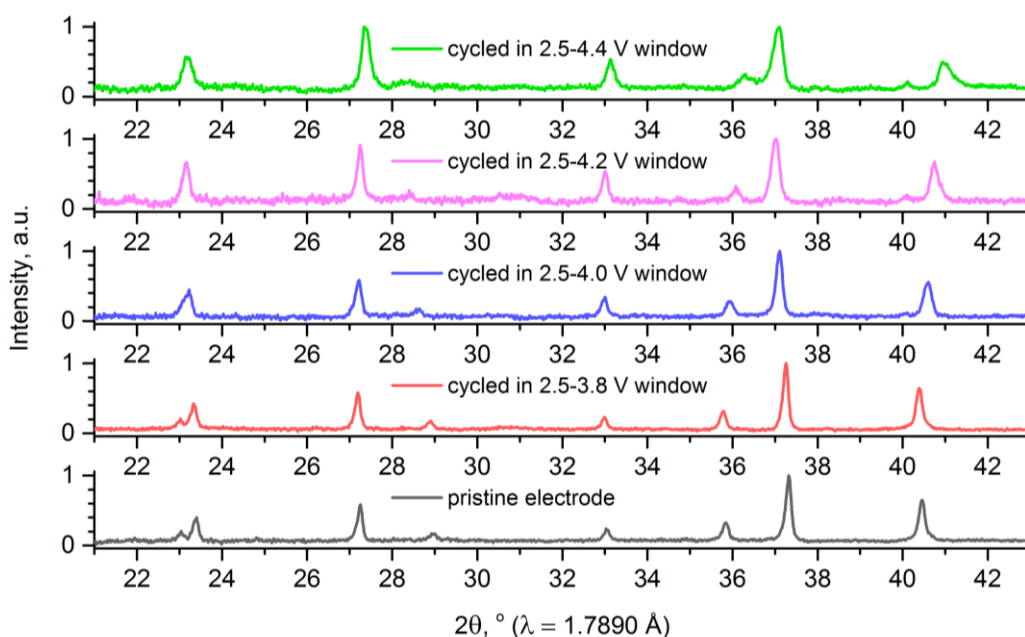
- The author agrees with the reviewer that the used synthesis method can influence the final product uniformity. In order to obtain more uniform samples stirring of the solution, mixing of the dried precursor and ball-milling between intermediate and high-temperature annealing stages were employed. In comparison with solid-state approach this method resulted in samples with higher phase uniformity. Hydrothermal synthesis of the NASICON-type cathode materials without following high-temperature annealing has not yet reported. As a further improvement of the used methodology cryochemical, aerosol, ultrasound stages may be used, however they add complexity to the sample preparation, and the actual synthesis route was chosen as an optimal compromise.

### Comment 10.

Have you observed the NASICON phase dispersion (due to volume changes on intercalation and de-intercalation) for long cycling? Have you found that SEI layers interfere as much as in the case of Li-containing ion batteries?

### Reply 10

- Our *ex situ* XRD data of  $\text{Na}_4\text{MnV}(\text{PO}_4)_3$  electrodes cycled 10 times in different potential windows shows very little phase degradation for cycling in 2.5-3.8V window. Cycling in extended potential window leads to widening of the Bragg reflections, which might be attributed to phase dispersion.



- Our EIS data results cannot attribute capacity degradation in extended potential window only to CEI layers. However analysis of these X-ray and electrochemical data is ongoing and requires further studies.

### Comment 11.

Have you ever observed amorphization of your materials or amorphous phase presence (I am suspicious about that when looking at Fig. 4.2, for example)? If you use vanadates or phosphates, it becomes highly possible. What could happen in this context for the NASICON mixed phases?

### Reply 11

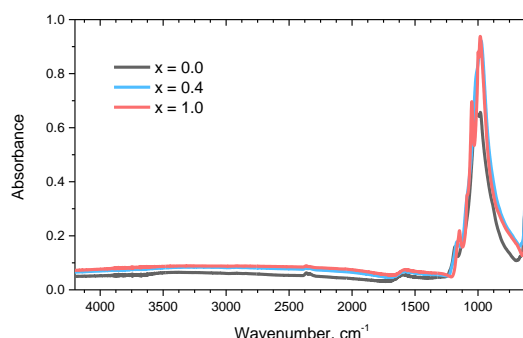
- The  $\text{Na}_{3+x}\text{Mn}_x\text{V}_{2-x}(\text{PO}_4)_3$  materials contain amorphous carbon phase, which plays a role of conductive coating and may be revealed at SEM images (Fig. 4.2, for example). Our ex situ XRD data of  $\text{Na}_4\text{MnV}(\text{PO}_4)_3$  electrodes cycled 10 times in different potential windows presented above shows a decrease in signal to noise ratio, however quantitative determination of the amorphous phase presence by X-ray diffraction, and the possible increase of its fraction due to NASICON phase amorphization during cycling requires using the standards; these experiments are planned for the future work.

### Comment 12.

Have you analyzed if the NASICON phases possess some residuals from their solution prehistory like the presence of water “impurities”, OH- etc.? Could they have any influence on the obtained data? If you analyze the carbon content by TGA (how exactly?), have you ever seen the presence of such residuals near 100°C or higher? Usually, such derivatives could influence phase transitions and could be stable at relatively high temperatures.

### Reply 12

- We analyzed our samples with TGA and ATR-FTIR. These results indicate only a minor (~1%) presence of water residuals in the studied samples based on the weight loss near 100°C and on the absence of absorption bands in the 3600-3100  $\text{cm}^{-1}$  range. Moreover, partial replacement of the phosphate groups with hydroxyl groups in hydrothermally-prepared  $\text{LiFePO}_4$  showed drastic degradation of the electrochemical capacity (<https://doi.org/10.1021/acs.chemmater.9b00627>), which we do not observe in the case of NASICON samples.



The corrections to the Chapter 3:

*The carbon content in the resultant products was measured by thermogravimetric analyzer Netzsch STA 449 F3 Jupiter under Ar:O<sub>2</sub> (80:20) flow at 10 K min<sup>-1</sup> heating rate in corundum crucible with lids. Empty crucible was used as a reference sample.*

The corrections to the Chapter 4:

The carbon content in the resultant samples was about 10% (Fig. 4. 2) as measured by thermogravimetric analysis.

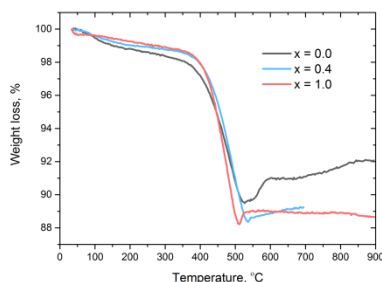


Fig. 4. 2 Thermogravimetric curves of the as-synthesized  $\text{Na}_{3+x}\text{Mn}_x\text{V}_{2-x}(\text{PO}_4)_3$  powders in air.

## Dr. Daniil Itkis

---

### Comment 13

As a comment for future, I would suggest the author think of the chemical reasons for manganese to promote performance degradation while expanding the solid-solution region for the considered compounds and enhancing the specific energy.

### Reply 13

- The author agrees with the reviewer that finding the reasons for manganese to modify in various ways the properties of the considered compounds is one of the major issues remaining for further studies of  $\text{Na}_{3+x}\text{Mn}_x\text{V}_{2-x}(\text{PO}_4)_3$  and other NASICON-type materials. We continue our work to unveil the relationships between redox behavior of transition metals, local effects related to Na or/and transition metal surroundings, potential ion-vacancy configurations, possible charge disproportionation and ordering, interfacial effects, etc.

## Prof. Seung-Taek Myung

---

The below is my comments for better understanding the thesis.

### Comment 14

Structural parameters of  $\text{Na}_{3+x}\text{Mn}_x\text{V}_{2-x}(\text{PO}_4)_3$  were present in Table 4.1. It would be better to explain how to calculate the lattice parameters such as least square method or Rietveld refinement of XRD data. With increasing the Mn content, the structural parameters were altered, namely, increase in the a-axis value but decrease in the c-axis parameter. What would be the most plausible reason for the decrease in the c-axis parameters.

### Reply 14

- The author thanks the reviewer for the compelling question. In order to account for why as  $\text{V}^{3+}$  is substituted with  $\text{Mn}^{2+}$  the a-axis is increased, but the c-axis is

decreased the Chapter 4 was expanded with:

Rising the  $Mn^{2+}$  content leads to the  $a$  parameter increase,  $c$  parameter decrease and an overall growth of the unit cell volume ( $V$ ). The increase of the  $a$  parameter is due to the replacement of smaller  $V^{3+}$  cations with larger  $Mn^{2+}$  (ionic radii are 0.64 Å and 0.83 Å, respectively) [128], which increases the average  $[O_3NaO_3(V/Mn)O_3NaO_3]$  column diameter, in addition to incorporation of neutralizing excess of  $Na^+$  cations into Na2 sites, which increase the intercolumn distance (Chapter, Fig. 2. 1). The decrease of the  $c$  parameter could be related to the weakening of the  $TM^{n+}-TM^{n+}$  and  $Na^+-TM^{n+}$  electrostatic repulsions [71]. Due to a steep rise of the parameter  $a$  (and a slight fall of the parameter  $c$ ) the 110 and 104 reflections positions show an evident inter-change as  $Mn^{2+}$  content increases.

### Comment 15

Associated with the Mn incorporation, it is too early to judge that the introduced Mn is divalent in Table 4.1. Confirmation of  $Mn^{2+}$  is necessary to express that “the replacement of smaller  $V^{3+}$  cation with larger  $Mn^{2+}$ ” in Page 59 line 7. The description is speculative before showing that Mn is divalent. Addition of XPS or XANES data is required to support the author’s assumption.

### Reply 15

- The author thanks the reviewer for this comment. The data on Mn oxidation state in two as-synthesized  $Na_{3+x}Mn_xV_{2-x}(PO_4)_3$  samples was added.

Chapter 4:

The XAS and XPS spectra confirming that Mn is divalent in the as-prepared samples are shown in Fig. A 2.

Appendices A:

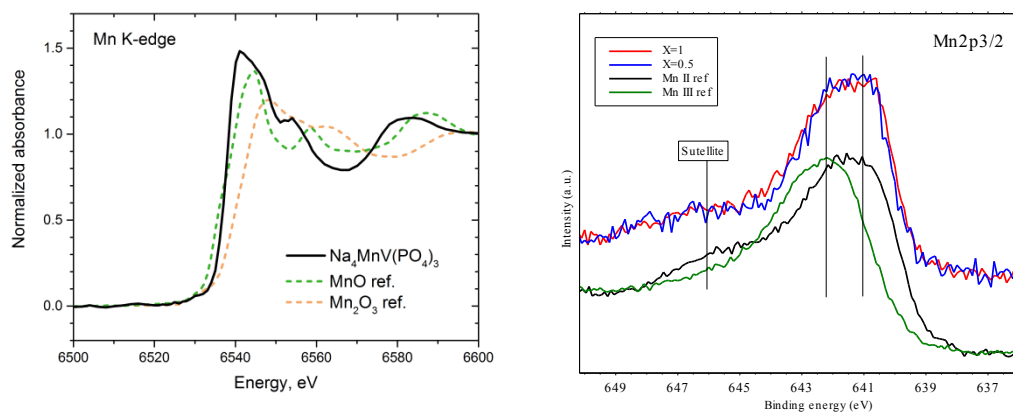


Fig. A 2 X-ray absorption spectra of the  $Na_4MnV(PO_4)_3$  powder at the K-edge of Mn (left) and  $Mn2p_{3/2}$  X-ray photoelectron spectra of the  $Na_{3.5}Mn_{0.5}V_{1.5}(PO_4)_3$  and  $Na_4MnV(PO_4)_3$  powders (right) with the  $Mn^{2+}$  and  $Mn^{3+}$  standards.

### Comment 16

It would be better to add visualized image for Na1 and Na2 sites for the  $Na_{3+x}Mn_xV_{2-x}(PO_4)_3$ , particularly, for the case of  $Na_4MnV(PO_4)_3$ .

### Reply 16

- The author agrees with the reviewer that visualized images of the Na1 and Na2

sites would be helpful for the understanding of the degree of the changes in NASICON structure with Mn substitution.

The text was added to the Chapter 4 and to the Appendices A:

*The changes in the NASICON framework caused by  $Mn^{2+}$  substitution are presented in () and Fig. A 3.*

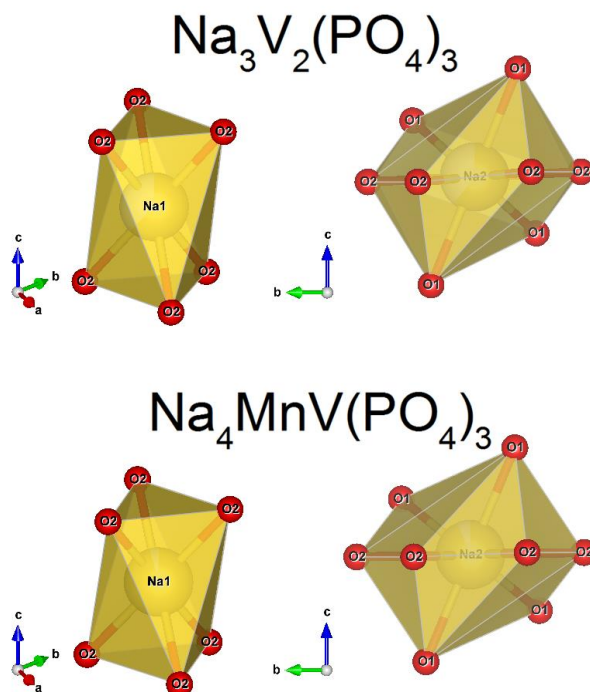


Fig. A 3 Na1 and Na2 polyhedra structures in the as-synthesized  $Na_{3+x}Mn_xV_{2-x}(PO_4)_3$  ( $x=0$  and 1)

### Comment 17

Page 65, line, 5. Electronic conductivity was speculated that carbon coating may improve the conductivity. Do you have more specific experimental data on the conductivity as a function of Mn content?

### Reply 17

- The author thanks the reviewer for this comment. The text in question is related to the electronic conductivity of the composite electrodes, but not of the  $Na_{3+x}Mn_xV_{2-x}(PO_4)_3$  bulk itself. Carbon coating improves electron transfer from the electrode material particles to the current collector. The relation between bulk-conductivity of the  $Na_{3+x}Mn_xV_{2-x}(PO_4)_3$  samples as a function of the Mn content  $x$  could be a topic of further work.

### Comment 18

Operando XRD data in Chapter 6. The illustrated images are too small to see it. Such good data should be enlarged for better view.

### Reply 18

- The author thanks the reviewer for this constructive comment. In order to improve

the clarity of the operando data presentation the figure 6.1 was expanded and placed together with the figure 6.2 on one landscape-mode page. The figures 6.3 and 6.6 were enlarged.

### Comment 19

Diffusivity in Fig. 7. 6. Whenever diffusivity is mentioned, the associated phase should be considered to avoid misinterpretation. For a single-phase reaction, it is easy to discuss kinetics; however, for a biphasic reaction, it would be very careful to separate the diffusivity depending on the dominant phase because the diffusion occurs in presence of two phases. Then, the measured diffusivity belongs to the Na-poor phase or Na-rich one? Also the plots should be compared as a function of Na content to compare the behavior with phase transitions.

### Reply 19

- The author agrees that the diffusivity values in the two-phase regions are not applicable due to the irrelevance of the Fick's law in the presence of two phases. Therefore the apparent diffusion coefficients were determined only in the single-phase regions, which are very narrow for the  $\text{Na}_3\text{V}_2(\text{PO}_4)_3$  material and increase progressively toward the  $\text{Na}_4\text{MnV}(\text{PO}_4)_3$  end-member. The notations of the Na-rich and Na-poor regions were added to the Fig. 7.6 to the right and left of the line indicating the phase transformation potential. Also the diffusivity was plotted as a function of Na content.

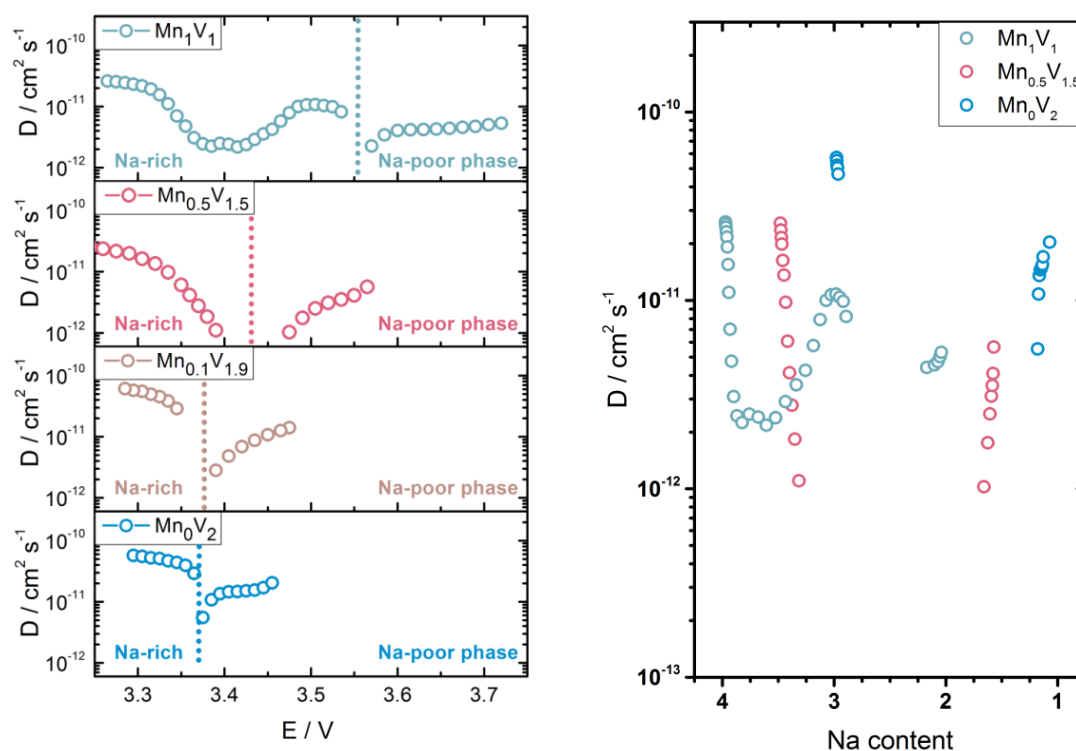


Fig. 7. 1 Apparent diffusion coefficients for  $\text{Mn}_0\text{V}_2$ ,  $\text{Mn}_{0.1}\text{V}_{1.9}$ ,  $\text{Mn}_{0.5}\text{V}_{1.5}$  and  $\text{Mn}_1\text{V}_1$  materials as determined from PITT data in the single-phase regions as a function of formal potential (left) and of Na content (right). Dashed line indicates the phase transformation potential.

### **Comment 20**

Typos. Please check chemical compositions to express numbers as subscript in Bibliography.

#### **Reply 20**

- The author thanks the reviewer for the comment. The subscripts, superscripts and duplicates were corrected in Bibliography.

## **Dr. Anatoliy Senyshyn**

---

There were a few minor remarks, which, however, do not put the scientific quality and novelty of the work in question:

### **Comment 21**

What was the purity and source of metallic sodium used in electrochemical cells? Was the lab distillation performed?

#### **Reply 21**

- The condition of metallic electrode is indeed important for the electrochemical properties of electrochemical cells due to high reactivity of alkali metals. Metallic sodium ( $\geq 99.8\%$ ) was obtained from Sigma-Aldrich and was used as received without lab distillation. The procedure of additional cleaning was included in the Chapter 3.2.

*During assembling of the electrochemical cells in a glovebox metallic sodium was additionally cleaned by slicing off the unreacted shiny part of a sodium piece followed by its rolling and further polishing immediately before clamping the electrochemical cell.*

### **Comment 22**

P.113: it is not fully clear how the linear range in current transients displayed in Fig. 7.10b were found/performed

#### **Reply 22**

- In order to clarify this point the following description was added:

Chapter 7:

*The linear part is chosen in the region after the current maxima with the greatest slope.*

### **Comment 23**

The list of abbreviations is not complete, furthermore the puzzling small controversies with CEI vs. SEI abbreviations at p.108 need to be resolved.

#### **Reply 23**

- The author thanks the reviewer for the careful assessment. The SEI abbreviation remained in the figure related to the equivalent circuit used to fit the experimental impedance spectra. Now the controversy is resolved and the figure is corrected.

List of Abbreviations:

$\theta$  – State of discharge

$Mn_0V_2 - Na_3V_2(PO_4)_3$   
 $Mn_{0.1}V_{1.9} - Na_{3.1}Mn_{0.1}V_{1.9}(PO_4)_3$   
 $Mn_{0.5}V_{1.5} - Na_{3.5}Mn_{0.5}V_{1.5}(PO_4)_3$   
 $Mn_1V_1 - Na_4MnV(PO_4)_3$   
*CEI – cathode/electrolyte interface*  
*R<sub>CEI</sub> – resistance of surface layers*  
*C<sub>CEI</sub> – capacitance of surface layers*  
*R<sub>ct</sub> – charge transfer resistance*  
*Ω – Ohm*  
*C<sub>dl</sub> – double layer capacitance*  
*η – overvoltage*

## Prof. Shinichi Komaba

---

No corrections were requested.

## Prof. Alexander Korsunsky

---

### Comment 24

In each case, specific information should be provided regarding the location, timing and experimental team composition, as well as task allocation between members.

### Reply 24

- The author thanks the reviewer for the suggestion. An Author's Contribution section was added after the List of Publications, where the main team composition is mentioned. Other team members are referred to in the Acknowledgements section.

### Author's Contribution

1. *The author is mainly responsible for this work. The author performed the synthesis of the materials, their structural, morphological and electrochemical characterization, analyzed and visualized the data, wrote the original draft and submitted the manuscript.*

*The co-authors performed the TG analysis, the operando X-ray diffraction experiment at the ESRF, performed the sequential Rietveld refinement and the Rietveld refinement of selected patterns, as well as supervised the work.*

2. *The author is mainly responsible for this work. The author performed the synthesis of the materials, their structural, morphological and electrochemical characterization, the laboratory operando X-ray diffraction experiments, performed the sequential Rietveld refinement and the Rietveld refinement of selected patterns, analyzed and visualized the data, wrote the original draft and submitted the manuscript.*

*The co-authors performed the ATR-FTIR, ICP, EDX, XPS experiments, the operando X-ray diffraction experiment at the ESRF, as well as supervised the work.*

3. *The author performed the synthesis of the materials, their structural and morphological characterization, analyzed and visualized the data, contributed to the manuscript preparation.*

*The co-authors performed the electrochemical measurements and analyzed its results, wrote the original draft as well as supervised the work.*

- *The author participated in preparation of the XAS experiments; the co-authors performed the experiments, analyzed and visualized the data.*

### **Comment 25**

The candidate should provide a clear declarative statement of their identification of the novelty of the results obtained and reported.

### **Reply 25**

- The author thanks the reviewer for the suggestion. A Novelty section was added to the thesis after the Author's Contribution section.

#### *Novelty*

1. *NASICON-type  $\text{Na}_{3+x}\text{Mn}_x\text{V}_{2-x}(\text{PO}_4)_3$  ( $x = 0.1, 0.2, 0.4, 0.6, 0.8$ ) materials are obtained for the first time and their main structural and morphological properties are determined*
2. *The relationship between their chemical composition and electrochemical properties is found. The compositions with the highest energy density ( $x=0.8$ ) and the compositions with the highest cyclic stability ( $x=0.2, x=0.4$ ) are identified.*
3. *The kinetic properties of the  $\text{Na}_{3+x}\text{Mn}_x\text{V}_{2-x}(\text{PO}_4)_3$  electrodes are studied. It is found that introduction of Mn adds to NASICON's tolerance of high current rate loads.*
4. *The (de)intercalation mechanisms of Na in  $\text{Na}_{3+x}\text{Mn}_x\text{V}_{2-x}(\text{PO}_4)_3$  ( $x = 0.2, 0.4, 0.6, 0.8$ ) are revealed for the first time. The phase diagram V-Mn-Na is constructed, and the range of existence of solid solutions  $\text{Na}_{3+x}\text{Mn}_x\text{V}_{2-x}(\text{PO}_4)_3$  is demonstrated.*
5. *The evolution of the Mn and V oxidation states during charge and discharge of  $\text{Na}_4\text{MnV}(\text{PO}_4)_3$  is shown for the first time in operando mode.*

### **Comment 26**

I would encourage the candidate to populate the thesis with explicit statements regarding the degree of novelty of specific individual results and conclusions they draw from their analysis.

### **Reply 26**

- The novelty section should facilitate the assessment of the degree of novelty of the thesis. In the Chapter 8 the original results are reported in higher details and their analysis draws that

#### *Chapter 8*

*with proper choice of the substitutions in their composition, NASICON-type cathodes can show even higher utilization of reversibly cycled charge at high voltages.*

### **Comment 27**

In terms of the general scientific context, the candidate addresses the nature of the processes within the chosen class of cathode materials in terms of solid solution and phase transformation evolution during charging. The redox evolution of transition metal ions leads to lattice distortion and eventually lead to lattice structure changes that correspond to phase transformation. I find this aspect of the study most interesting: it seems to me that more can be done in this respect to

consider the thermodynamic driving forces for transformation based on the data collected by the candidate.

### **Reply 27**

- The author agrees with the reviewer on this point and, indeed, we continue analysis of the collected data as well as implement density functional theory and molecular dynamics studies of the  $\text{Na}_{3+x}\text{Mn}_x\text{V}_{2-x}(\text{PO}_4)_3$  compounds. Further studies are required to draw solid conclusions.

### **Comment 28**

I also note that phase transitions of the first and second kind are mentioned in the text – this would benefit from due explanation or discussion.

### **Reply 28**

- The author thanks the reviewer for the suggestion. The following part was added to the Chapter 2.3.6.

*According to Gibbs' phase rule, there can be zero degrees of freedom in the intensive variables in the two-phase regime of a two-component system (given constant temperature and pressure), which leads to the characteristic flat galvanostatic curve of phase-separating electrode materials such as  $\text{LiFePO}_4$  or  $\text{Na}_3\text{V}_2(\text{PO}_4)_3$  during alkali ion (de)intercalation. Materials, forming single-phase solid-solutions over wide alkali ion concentration range, are characterized by sloping potential-composition curves. However, a sloping voltage curve may also originate from a wide size distribution of materials' particles each undergoing a phase transition [92], which adds to the non-triviality of such systems' thermodynamics. The first-order phase transitions may arise from various reasons such as charge ordering, particularities of electronic structure, possible charge disproportionation or interfacial effects [93]. Understanding the mechanism of (de)intercalation is highly relevant to the thermodynamics and kinetics of battery materials and is important for the improvement of their properties like specific energy and power density. While a great number of research is published on the Li insertion mechanism in  $\text{LiFePO}_4$ , not that many studies are devoted to the Na insertion mechanisms in NASICON-type electrode materials.*

The author feels the quality of the manuscript has been significantly improved and would like to thank all jury members for the careful review of the thesis